A Volcanic Seismic Activity Morphism to Collect Data from the Cotopaxi Volcano

T. Sunitha [1], Dr.T. Nedunchezhian [2], Dr.G. Vijaya Kumar [3], B. Neelima [4], Mrs.B.Malleswari [5]
[1, 2, 3, 4]Department of Computer Science and Engineering,
[5]Electronics and Communications Engineering,
[1, 2, 3, 4, 5] QIS College of Engineering and Technology, Ongole, Andhra Pradesh, India
thella.sunitha@qiscet.edu.in[1], nedunchezhian.t@qiscet.edu.in [2], vijayakumar.g@qiscet.edu.in[3], neelima.b@qiscet.edu.in[4], malleswari.b@qiscet.edu.in[5]
Corresponding Author Mail: qispublications@qiscet.edu.in

***Abstract*: Area Under the receiver operating characteristic Curve (AUC) is used to improve categorization for long period (LP) and volcano tectonic (VT) seismic events, this paper suggests a novel volcanic seismic signal descriptor. In place of traditional seismic signal processing techniques like frequency or scale analysis, it uses image processing techniques to depict a volcanic seismic incident from a unique and unusual angle. The suggested descriptor enables exploration of the seismic signal space to identify event patterns, followed by texture-based extraction of shape and intensity features into numeric vector output to feed a collection chosen various taxonomies with machine learning classifiers. Here, descriptor was tested using a database of 637 Seismic activity from the Cotopaxi volcanoes, including VT, LP, and further types of Seismic actions (e.g., ice quakes or rock fall). AUC values of 0.95 and 0.96 were obtained using a feed forward back propagation for the classifier of artificial neural network on two investigational datasets which encloses feature vector representation of signals neither and nor event switching, correspondingly. An accurate value of 96 percentile would be acquired with the purpose of the occurrence patterns by using the database of signals. These collected findings shows that the suggested descriptor was capable to produce enough Seismic Signal Representations for various feature spaces and here output offers uncertain outcomes in the categorization of Seismic Events of Volcano.**

Keywords— Spectrogram based Features, Seismic Event Classification, Machine Learning Classifiers (MLCs), Seismic Pattern Generation.

I. INTRODUCTION

To identify behavioral changes offer initial notices for the events which are impending volcanic activity, comprehensive monitoring of volcanoes are essential. To completely comprehend a volcano's behavior, volcanic gases, seismicity, rocks, ground motions, satellite photos and water chemistry shall be examined [1]. While extensive monitoring networks with a variety of equipment are necessary to give information on potential volcanic unrest, seismicity offers valuable insight into the inside movement of volcanoes. Many Machine Learning Classifiers (MLCs) had been employed in literature to solve the pattern recognition issue connected to the detection of various volcanic activity-related seismic signals. In order to

decrease the dimensions from the given data and improve distinction of a class, various approaches of machine learning which are typical to use some of the alternative depiction of the information through respect to the novel space. This representation have been obtained by mining important features from the novel signal. Volcanic-seismic signals have historically been automatically classified using parameters relating to certain properties from the frequency, temporal, and/or scale and cepstral domains [2]–[4]. Within the scale domains, certain bands that are utilized for frequency had been employed as features which were linked probably for the entropy or energy of the signals [6], [7], whereas statistical topographies, for example, explains behavior of the facts from distribution [2], [5], [6]. Although there are various possible representations of the data that may be utilized, their utility would depend on the situation at hand and the algorithm to be employed, making it as a persistent challenge to determine the best demonstration of seismic events for enhancing sorting performance.

By using image processing techniques rather than traditional seismic signal processing methods like scale analysis or frequency, is a suggested descriptor aims to portray volcanic seismic occurrences from a unique and diverse perspective. To calculate the collection of features like 17 from the texture, shape, intensity statistics etc., which were referred to be the output of descriptor, the pattern for seismic event is segmented firstly to a spectrogram picture which was of gray-level.

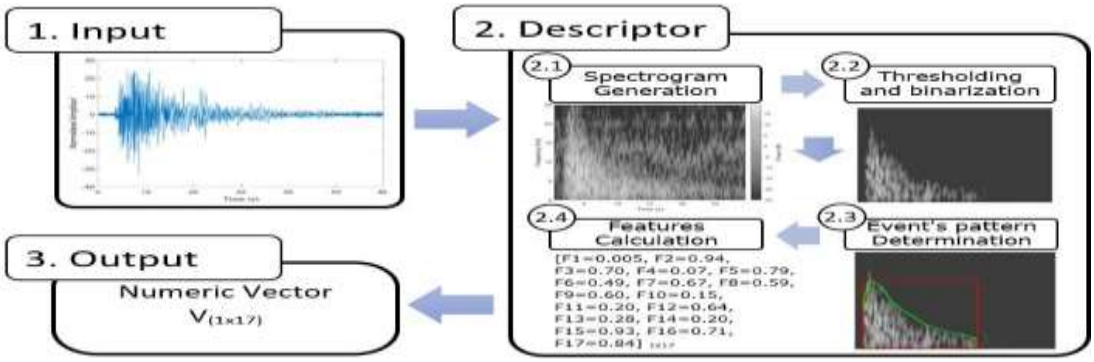

Figure I: Workflow for proposed descriptor.

The suggested descriptor, the chosen MLCs, and the various experimental setup used for the descriptor assessment are all described in depth in Section II. AUC totals acquired by the selected MLCs using the Wilcoxon statistical test [6], [7] for assessing the significance of the differences between the classification models, were used to determine the accuracy outcomes in seismic event pattern determination and also descriptor output authentication. Additionally, a preliminary comparison between the chosen MLCs and previously created methods that are documented in the literature is offered. In Section IV, findings and future work are summarized.

II. MATERIALS AND METHODS

A. *Seismic Signal Database*

The 637 seismic events in the database utilised for this paper consist of 560 samples from the LP class and 77 samples from the VT class. The Cotopaxi volcano in Ecuador, located at

(00.677 S, 78.436 W), was the source of all the data collected in the years 2012, 2013 January, 2014 January, 2018 January, between January 2019 and March 2019. Geophysical Institute of National Polytechnic School (IGEPN) tracks and analyzes the Ecuadorian seismic and volcanic activity, which contributed this database. The three-axial CMG-40T Guralp seismometer, whose sensitivity is 1600 V/ms1, and the 24-bit Geotech Smart 24-D digitizer, which samples at 50 Hz, were utilized in the broadband seismic acquisition system. According to its waveform, spectrogram, and location, each seismogram from this database represents a single distinct seismic event was manually recognized and categorized by IGEPN experts.

B. *Volcanic Seismic Signal Descriptor*

A specified ROI inside spectrogram picture is used to compute the intensive statistics, shape, and texture of the suggested descriptor, which describes numeric output vector from input signal. The suggested descriptor's process is depicted in Fig. 1, and each step's description is given below.

1) **Spectrogram Generation**: Short Time Fourier Transform (STFT) uses original signal to create the gray-level spectrogram pictures. In order to prevent information from being lost at the window's edge and to optimize the energy in the main body of the signal, this technique employed a Kaiser window with a 1.5-s sampling window size and 75% of overlapping data.
2) **Thresholding and Binarization**: In this phase, the gray-level spectrogram pictures are filtered using a threshold value of 0 dB that was obtained through experimentation (Figure. I step 2.2). This keeps seismic events which were related frequency components while removing the low-amplitude ones. The use of a power threshold assists in signal cleaning since the data gathering device (seismometers) is extremely sensitive, making it usual to have i^{th} pixel inside the contour and the sample x intensity is mainly the mean noise at various frequencies. By using Otsu's approach each grayscale picture was transformed into a binary image, which determines the ideal threshold for conversion by reducing the intra class variation between two hypothetical pixel classes (see Fig. 1 step 2.2).
3) The contour and bounding box of the AOI can be determined by using the seismic event in step three, "**Determination of the Event Pattern**." By using Jacob's halting criterion which served as the foundation for the contour computation [5] can be modified Moore-neighbor tracing algorithm. The other side, eight-connected components (object or blobs) approach was used to determine the bounding box (see Figure. I step 2.3, red line). By planting a seed (the initial pixel) and thoroughly scanning the eight associated pixels around in direction of a clockwise, it is determined to contour the objects in an image. This process checks to see if there have been any changes in the current pixel's intensity in relation to the seed.
4) **Feature calculation**: The segmented event patterns, a collection of features of 17

including shape, texture descriptors and intensity statistics were derived. These characteristics were combined to create a numerical vector, which is the suggested descriptor output. The chosen characteristics were evaluated based on previously published methods, which discovered that they may offer pertinent information in picture classification issues [5]–[7] (see Figure. 1 step 2.4 the green-line contour).

C. Classifiers based on machine learning

In the literature, a number of MLCs have been described for the categorization of seismic events. The most popular form of classifier appears to be most variations of the Support Vector Machine (SVM) technique, such as multiclass SVM [7] and SVM with linear kernel. Hidden Markov models, Decision trees [7], Artificial neural networks (ANNs) [6-7], evolutionary algorithms and, more recently, the Gaussian mixture model are other less often used techniques that have also shown satisfactory results. Therefore, five MLCs with various classifications (based on their functionality) would be taken into account, this paper for evaluating the suggested descriptor output fairly. The following description of the chosen MLCs. 1. The Naive Bayes (NB) classifier is originated on probability models with sturdy liberal expectations. The presupposed that c is a variable of class which depends on n input characteristics, including x_1, x_2... x_n. When characteristics are provided, the Bayer's theorem with constant denominator is uses forecast to the class variable c. (it does not depend on c).

2. Descriptor Output Quality: Here, test was designed for verifying to collect pertinent data and suggested descriptor output on the calibre of calculated features. In this way, the descriptor output was combined with five distinct MLCs are FFBP ANN, SVM, kNN, RF classifiers and NB. Following is a description of the test's exercise and test barriers, evaluation metrics and MLCs setup.

1) *Training and Test Partitions*: Before the classification stage, we specifically used the tenfold cross-validation approach to create disjoint training and test divisions. Individual MLCs will be educated on several training sets in this manner, gaining knowledge from various input space representations. The categorization of individual samples as a consequence of testing on these various sets varies.

2) Configuration of MLCs: The SVM classifier employed a kernel function calibrated to be linear, radial basis, polynomial, and sigmoid functions, and the regularization parameter C (cost) was optimized in the range from 10^{-4} to 10^{4} (growing by a factor of 10). When using the kNN classifier to determine the size of the neighborhood, an ideal value of k has to be estimated. The number of hidden layers in the FFBP neural network was calculated as n (attributes number of classes)/2. One layer of output connected to the binary classification (LP or VT). The sigmoid (hyperbolic tangent) function was used as the transfer function for all layers, and the number of iterations (epochs) was optimized in the range of 100 to 10,000 epochs with an interval increment of 500 units. The number of tree-based predictors included in the RF classifier was tuned to be between 100 and 1000.

(With an increment of ten units). With X being the total number of characteristics available in the current data set, each tree employed the log2(X) 1 to choose attributes at random. (version 3.6).

III. RESULTS

A. The Performance of Proposed Descriptor's

The perimeter (F_7), on the other hand, has less variance between the two types of occurrences for the group of characteristics based on form (ΔF_7 0.08). The cases that were taken into account led to this value. Even while it is feasible to see that the VT events have greater morphological values than the LP events, the breadth, which is dependent on the length of the event, does not behave in the same way. Therefore, despite the fact that both qualities typically have low values, there is not necessarily a link between them.

The contrast (F_{14}) and Second angular momentum (F_{13}) and emerged with the characteristics with reduced variance between two types of events within the collection of texture-based features (F_{13} 0.02 and F_{14} 0.07). These results were anticipated since there aren't many prominent gray-tone transitions in gray-level images, and the F_{13} assesses how homogenous an image's intensity is. Similar to the F_{14} feature, gray-level pictures have no bearing on the degree of local strength fluctuation exhibited in image.

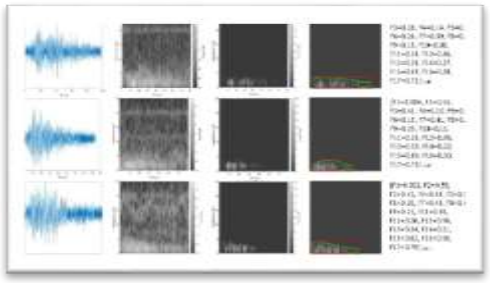

Figure. 2: To show results of the Performance of Proposed Descriptor's

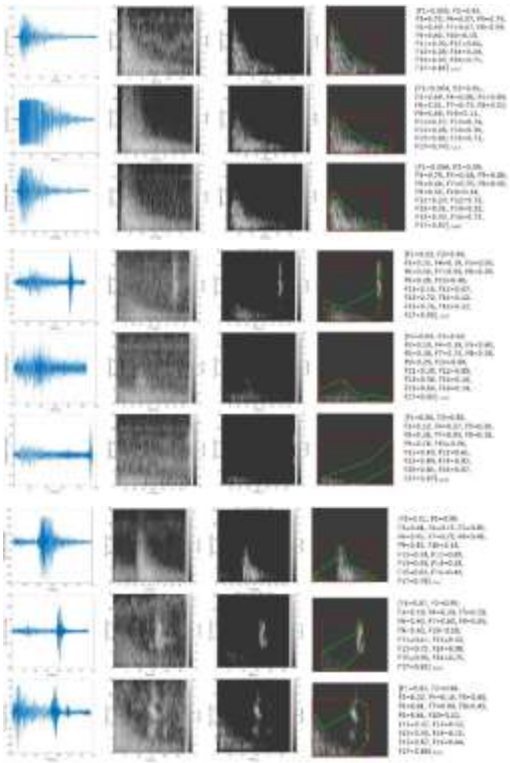

B. Descriptor Output's Quality

On two experimental data sets, we used five different MLCs to assess the descriptor output. The first (D1) was created using 598 instances of numerical vectors (descriptor outputs) that were derived from input signals but did not contain overlapping seismic events. Second (D2), which has 637 instances, constructed using all of the numerical vectors from the D1 data set as well as additional numerical vectors that were taken from signals of input that had overlapping events of seismic signals (i.e., 39 additional occurrences including 32 LP and 7 VT events). The following is a description of the MLCs' outcomes.

1) NB Classifier Performance
2) SVM Classifier Performance

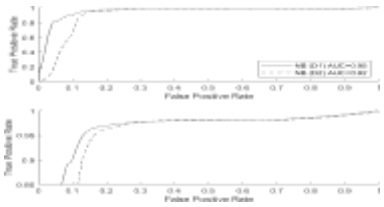

Figure 6: Top graph ROC curve and bottom graph part of the ROC curve with an AUC ≥ 0.85.

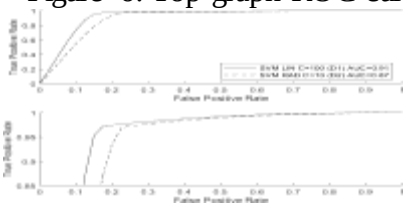

Figure 7: Top graph ROC curve and bottom graph part of the ROC curve with an AUC ≥ 0.85

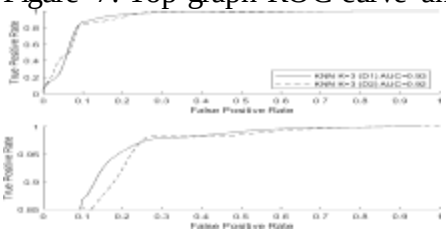

Figure. 8. Top graph ROC curve and bottom graph part of the ROC curve with an AUC ≥ 0.85

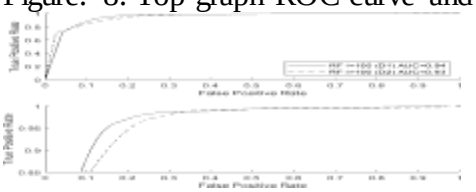

Figure. 9: Top graph ROC curve and bottom graph part of the ROC curve with an AUC ≥ 0.85

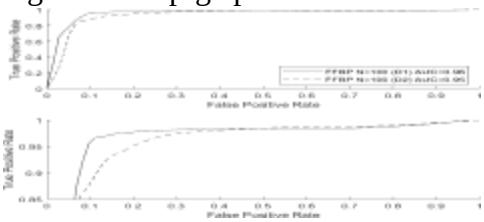

Figure 10: Top graph ROC curve and bottom graph z part of the ROC curve with an AUC ≥ 0.85.

3) Performance of kNN Classifier: These outcomes were attained by applying the number of K 3 neighbors same model. To resolve overlapping of signal issue in the data set D2 it was shown statistically insignificant.
4) Performance of the RF Classifier: On both sets of data, this classifier performed similarly in terms of classification at p 0.05 As a result, the performance of this classifier is not considerably impacted by the descriptor's response to signal overlapping. Due to the positive findings, it is feasible to determine that the suggested descriptor provides adequate results when employed in conjunction with this classifier.

IV. CONCLUSION AND NEXT WORK

In order to increase AUC scores for the categorization of LP and VT seismic events, we suggest a novel volcanic seismic signal descriptor in this study. New descriptor represents the volcano seismic event signals from a novel and innovative perspective that uses image processing techniques rather than traditional seismic signal processing techniques like frequency or scale analysis. There are two steps to the descriptor validation process. All of the MLCs had successful outcomes, as determined by the AUC measure. The overlapping seismic events in the D2 data set were particularly sensitive to this classifier's performance. It also shows that the proposed descriptor is invariant across various MLCs. Plans exist to incorporate two substantial upgrades to the suggested description as future work.

REFERENCES

[1] U. S. Geological-Survey. *Volcano Hazards Program*. Accessed: May 18, 2019. [Online]. Available: https://volcanoes.usgs.gov/vhp/ monitoring.html

[2] M. Malfante, M. Dalla Mura, J.-P. Metaxian, J. I. Mars, O. Macedo, and A. Inza, "Machine learning for volcano-seismic signals: Challenges and perspectives," *IEEE Signal Process. Mag.*, vol. 35, no. 2, pp. 20–30, Mar. 2018.

[3] R. Soto, F. Huenupan, P. Meza, M. Curilem, and L. Franco, "Spectro-temporal features applied to the automatic classification of volcanic seismic events," *J. Volcanol. Geotherm. Res.*, vol. 358, pp. 194–206, Jun. 2018. [Online]. Available: http://www.sciencedirect. com/science/article/pii/S0377027318300301

[4] Y. Rizk, H. Partamian, and M. Awad, "Toward real-time seismic feature analysis for bright spot detection: A distributed approach," *IEEE J. Sel. Topics Appl. Earth Observat., Remote Sens.*, vol. 11, no. 1, pp. 322–331, Jan. 2018.

[5] M. Curilem *et al.*, "Improving the classification of volcanic seismic events extracting new seismic and speech features," in *Progress in Pat- tern Recognition, Image Analysis, Computer Vision, and Applications*, M. Mendoza and S. Velastín, Eds. Cham, Switzerland: Springer, 2018, pp. 177–185.

[6] Z. Zhang and E. Sejdić, "Radiological images and machine learning: Trends, perspectives, and prospects," *Comput. Biol. Med.*, vol. 108, pp. 354–370, May 2019. [Online]. Available: http://www.sciencedirect. com/science/article/pii/S0010482519300642

[7] R. Lara-Cueva, D. S. Benitez, V. Paillacho, M. Villalva, and J. L. Rojo-Alvarez, "On the use of multi-class support vector machines for classification of seismic signals at cotopaxi volcano," in Proc. IEEE Int. Autumn Meeting Power, Electron. Comput. (ROPEC), Nov. 2017, pp. 1–6.

[8] J. C. Lahr, B. A. Chouet, C. D. Stephens, J. A. Power and R. A. Page, "Earthquake classification location and error analysis in a volcanic environment: Implications for the magmatic system of the 1989–1990 eruptions at Redoubt volcano Alaska", *J. Volcanol. Geotherm. Res.*, vol. 62, no. 1–4, pp. 137-151, 1994.

[9] K. Aki, M. Fehler and S. Das, "Source mechanism of volcanic tremor: Fluid-driven crack models and their application to the 1963 Kilauea eruption", *J. Volcanol. Geotherm. Res.*, vol. 2, no. 3, pp. 259-287, 1977.

[10] B. Chouet, "Resonance of a fluid-driven crack: Radiation properties and implications

for the source of long-period events and harmonic tremor", J. Geophys. Res. Solid Earth, vol. 93, no. B5, pp. 4375-4400, 1988.

[11] J. Neuberg, R. Luckett, B. Baptie and K. Olsen, "Models of tremor and low-frequency earthquake swarms on Montserrat", J. Volcanol. Geotherm. Res., vol. 101, no. 1, pp. 83-104, 2000.

[12] E. Del Pezzo, F. Bianco and I. Borgna, "Magnitude scale for lp events: A quantification scheme for volcanic

[13] B. A. Chouet and R. S. Matoza, "A multi-decadal view of seismic methods for detecting precursors of magma movement and eruption", J. Volcanol. Geotherm. Res., vol. 252, no. suppl. C, pp. 108-175, 2013.

[14] B. A. Chouet, "Long-period volcano seismicity: Its source and use in eruption forecasting", Nature, vol. 380, no. 6572, pp. 309-316, Mar. 1996.

[15] S. McNutt, "Volcanic tremor", Encyclopedia Earth Syst. Sci., vol. 4, pp. 417-425, 1992.

[16] A. J. Hotovec, S. G. Prejean, J. E. Vidale and J. Gomberg, "Strongly gliding harmonic tremor during the 2009 eruption of Redoubt volcano", J. Volcanol. Geotherm. Res., vol. 259, no. suppl. C, pp. 89-99, 2013.

[17] S. R. McNutt and T. Nishimura, "Volcanic tremor during eruptions: Temporal characteristics scaling and constraints on conduit size and processes", J. Volcanol. Geotherm. Res., vol. 178, no. 1, pp. 10-18, 2008.

[18] P. Traversa, O. Lengliné, O. Macedo, J.-P. Métaxian, J.-R. Grasso, A. Inza, et al., "Short term forecasting of explosions at Ubinas volcano Perú", J. Geophys. Res.: Solid Earth, vol. 116, no. B11, 2011.

[19] M. Iguchi, H. Yakiwara, T. Tameguri, M. Hendrasto and J. I. Hirabayashi, "Mechanism of explosive eruption revealed by geophysical observations at the Sakurajima Suwanosejima and Semeru volcanoes", J. Volcanol. Geotherm. Res., vol. 178, no. 1, pp. 1-9, 2008.

[20] T. H. Druitt, S. R. Young, B. Baptie, C. Bonadonna, E. S. Calder, A. B. Clarke, et al., "Episodes of cyclic vulcanian explosive activity with fountain collapse at Soufrière Hills volcano Montserrat", Geol. Soc. London Memoirs, vol. 21, no. 1, pp. 281-306, 2002.

[21] T. Ohminato, M. Takeo, H. Kumagai, T. Yamashina, J. Oikawa, E. Koyama, et al., "Vulcanian eruptions with dominant single force components observed during the Asama 2004 volcanic activity in Japan", Earth Planet. Space, vol. 58, no. 5, pp. 583-593, May 2006.

[22] L. A. Inza, J.-P. Métaxian, J. I. Mars, C. J. Bean, G. S. O'Brien, O. Macedo, et al., "Analysis of dynamics of vulcanian activity of Ubinas volcano using multicomponent seismic antennas", *J. Volcanol. Geotherm. Res.*, vol. 270, no. suppl. C, pp. 35-52, 2014.

[23] S. Haykin, V. Tresp and J. A. Benediktsson, "Big data: Practical applications [Scanning the Issue]", *Proc. IEEE*, vol. 104, no. 11, pp. 2082-2084, Nov. 2016.

[24] . Zaugg, M. Van Der Schaar, L. Houégnigan, C. Gervaise and M. André, "Real-time acoustic classification of sperm whale clicks and shipping impulses from deep-sea observatories", *Appl. Acoust.*, vol. 71, no. 11, pp. 1011-1019, 2010.

[25] N. C. Han, S. V. Muniandy and J. Dayou, "Acoustic classification of Australian anurans based on hybrid spectral-entropy approach", *Appl. Acoust.*, vol. 72, no. 9, pp. 639-645, 2011.

[26] P Ramprakash, M Sakthivadivel, N Krishnaraj, J Ramprasath. "Host-based Intrusion Detection System using Sequence of System Calls" International Journal of Engineering and Management Research, Vandana Publications, Volume 4, Issue 2, 241-247, 2014

[27] N Krishnaraj, S Smys."A multihoming ACO-MDV routing for maximum power efficiency in an IoT environment" Wireless Personal Communications 109 (1), 243-256, 2019.

[28] N Krishnaraj, R Bhuvanesh Kumar, D Rajeshwar, T Sanjay Kumar, Implementation of energy aware modified distance vector routing protocol for energy efficiency in wireless sensor networks, 2020 International Conference on Inventive Computation Technologies (ICICT),201-204

[29] Ibrahim, S. Jafar Ali, and M. Thangamani. "Enhanced singular value decomposition for prediction of drugs and diseases with hepatocellular carcinoma based on multi-source bat algorithm based random walk." Measurement 141 (2019): 176-183. https://doi.org/10.1016/j.measurement.2019.02.056

[30] Ibrahim, Jafar Ali S., S. Rajasekar, Varsha, M. Karunakaran, K. Kasirajan, Kalyan NS Chakravarthy, V. Kumar, and K. J. Kaur. "Recent advances in performance and effect of Zr doping with ZnO thin film sensor in ammonia vapour sensing." GLOBAL NEST JOURNAL 23, no. 4 (2021): 526-531. https://doi.org/10.30955/gnj.004020 , https://journal.gnest.org/publication/gnest_04020

[31] N.S. Kalyan Chakravarthy, B. Karthikeyan, K. Alhaf Malik, D.Bujji Babbu,. K. Nithya S.Jafar Ali Ibrahim , Survey of Cooperative Routing Algorithms in Wireless Sensor Networks, Journal of Annals of the Romanian Society for Cell Biology ,5316-5320, 2021

[32] Rajmohan, G, Chinnappan, CV, John William, AD, Chandrakrishan Balakrishnan, S, Anand Muthu, B, Manogaran, G. Revamping land coverage analysis using aerial satellite image mapping. Trans Emerging Tel Tech. 2021; 32:e3927. https://doi.org/10.1002/ett.3927

[33] Vignesh, C.C., Sivaparthipan, C.B., Daniel, J.A. et al. Adjacent Node based Energetic Association Factor Routing Protocol in Wireless Sensor Networks. Wireless Pers Commun 119, 3255–3270 (2021). https://doi.org/10.1007/s11277-021-08397-0.

[34] C Chandru Vignesh, S Karthik, Predicting the position of adjacent nodes with QoS in mobile ad hoc networks, Journal of Multimedia Tools and Applications, Springer US,Vol 79, 8445-8457,2020